Enhancement of superconductivity in La_{1−x}Sm_{x}O_{0.5}F_{0.5}BiS_{2}

Y. Fang, D. Yazici, B. D. White, and M. B. Maple

Phys. Rev. B **91**, 064510 — Published 24 February 2015

DOI: 10.1103/PhysRevB.91.064510

Enhancement of Superconductivity in $La_{1-x}Sm_xO_{0.5}F_{0.5}BiS_2$

Y. Fang[2,3], D. Yazici[1,2], B. D. White[1,2], and M. B. Maple[1,2,3,*]
[1]*Department of Physics, University of California, San Diego, La Jolla, California 92093, USA*
[2]*Center for Advanced Nanoscience, University of California, San Diego, La Jolla, California 92093, USA and*
[3]*Materials Science and Engineering Program, University of California, San Diego, La Jolla, California 92093, USA*

The superconducting and normal-state properties of $La_{1-x}Sm_xO_{0.5}F_{0.5}BiS_2$ ($0.1 \leqslant x \leqslant 0.9$) have been studied via electrical resistivity, magnetic susceptibility, and specific heat measurements. By using suitable synthesis conditions, Sm exhibits considerable solubility into the $CeOBiS_2$-type $LaO_{0.5}F_{0.5}BiS_2$ lattice. In addition to a considerable enhancement of the superconducting volume fraction, it is found that the superconducting transition temperature T_c is dramatically enhanced with increasing Sm concentration to 5.4 K at x = 0.8. These results suggest that T_c for $SmO_{0.5}F_{0.5}BiS_2$ could be as high as $\sim$6.2 K and comparably high T_c values might also be obtained in the compounds $LnO_{0.5}F_{0.5}BiS_2$ (*Ln* = Eu - Tm) if they can be synthesized.

PACS numbers: 74.25.F-, 74.25.Dw, 74.62.Bf

I. INTRODUCTION

Since the discovery of superconductivity in $Bi_4O_4S_3$,[1,2] a tremendous amount of effort has been made to synthesize new superconducting materials with BiS_2-layers. Through fluorine substitution for oxygen, the compounds $LnO_{1-x}F_xBiS_2$ (*Ln* = La, Ce, Pr, Nd, Yb) were soon reported to have superconducting transition temperatures, T_c, ranging from 2 to 10 K.[3–10] Superconductivity can also be induced in $LaOBiS_2$ via substitution of tetravalent elements, such as Th^{4+}, Hf^{4+}, Zr^{4+}, and Ti^{4+}, for trivalent Ln^{3+}.[11] Very recently, bulk superconductivity was observed in La substituted $SrFBiS_2$.[12] These compounds form in a tetragonal structure with space group *P4/nmm*, composed of alternate stacking of double superconducting BiS_2 layers and blocking *Ln*O or SrF layers.[3–5,7,11,12] Thus, there exists significant phase space to design and synthesize analogous superconductors by changing the chemical environment of the blocking layers or modifying the superconducting layers.

The T_c values for samples of the superconducting compounds $LnO_{1-x}F_xBiS_2$, prepared at ambient pressure, increase with increasing atomic number for *Ln* = La - Nd.[7,8] Non-superconducting samples of $LnBiOS_2$ (*Ln* = La, Ce, Pr, Nd, Sm, Gd, Dy, Yb) were successfully synthesized decades ago;[13] however, attempts to prepare fluorine-substituted samples of $LnBiO_{1-x}F_xS_2$ for *Ln* = Sm - Tm, which could potentially exhibit superconductivity, have been unsuccessful. Since the highest T_c in as-grown samples of $LaO_{1-x}F_xBiS_2$ is $\sim$2.8 K for x = 0.5, we felt that it would be instructive to systematically substitute Sm for La in $LaO_{0.5}F_{0.5}BiS_2$ in order to determine the solubility limit and to address the question of whether $SmO_{0.5}F_{0.5}BiS_2$ might be a superconductor.

In this paper, we report the evolution of superconductivity as well as the normal-state properties of polycrystalline samples with *nominal* chemical composition $La_{1-x}Sm_xO_{0.5}F_{0.5}BiS_2$ from x = 0.1 to the Sm solubility limit near x = 0.8. Evidence for an enhancement with x of both T_c and the volume fraction is presented. The increasing volume fraction suggests that high-quality samples of $SmO_{0.5}F_{0.5}BiS_2$ might exhibit bulk superconductivity if the phase could be stabilized. Performing a linear extrapolation of T_c vs. x to x = 1 allowed us to estimate $T_c \sim 6.2$ K for $SmO_{0.5}F_{0.5}BiS_2$. The results are consistent with the trend of T_c vs. *Ln* for the reported $LnO_{0.5}F_{0.5}BiS_2$ compounds. Until the heavy lanthanide variants can be synthesized, the results reported herein for *Ln* = Sm constitute a test case for a promising approach to make a preliminary assessment of superconductivity in $LnO_{0.5}F_{0.5}BiS_2$ compounds.

II. EXPERIMENTAL DETAILS

Polycrystalline samples of $La_{1-x}Sm_xO_{0.5}F_{0.5}BiS_2$ were synthesized by means of solid state reaction as described elsewhere.[7] Powder X-ray diffraction experiments were performed at room temperature using a Bruker D8 Discover x-ray diffractometer with Cu-K_α radiation. All resulting patterns were analyzed by Rietveld refinement using the GSAS+EXPGUI software package.[14,15] Electrical resistivity measurements were performed by means of a standard four-wire technique using a Linear Research LR700 ac impedance bridge and a home-built probe in a liquid ^{4}He Dewar from 300 K to $\sim$1.1 K. Alternating current (ac) magnetic susceptibility measurements were made down to $\sim$1.1 K in a liquid ^{4}He Dewar using home-built magnetic susceptibility coils and the Linear Research LR700 impedance bridge. Direct current (dc) magnetic susceptibility measurements were carried out using a Quantum Design Magnetic Properties Measurement System (MPMS). Specific heat measurements were performed in a Quantum Design Physical Property Measurement System (PPMS) Dynacool using a standard thermal relaxation technique.

III. RESULTS AND DISCUSSION

A representative XRD pattern for $La_{1-x}Sm_xO_{0.5}F_{0.5}BiS_2$ with x = 0.7 is shown in Fig. 1, plotted with its refined pattern for comparison. For $x \leqslant 0.8$, the main diffraction peaks can be fitted well by the Rietveld refinement method to a $CeOBiS_2$-type tetragonal crystal structure with space group *P4/nmm*. The refinement analysis demonstrates the presence of negligible secondary phases like La(Sm)O and

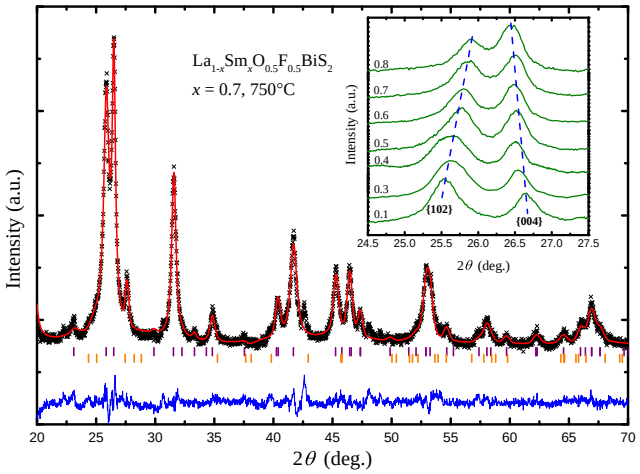

FIG. 1: (Color online) X-ray diffraction pattern of $La_{0.3}Sm_{0.7}O_{0.5}F_{0.5}BiS_2$ as a representative example. Black crosses denote the experimental data. Red and blue lines are the calculated XRD pattern and the difference between the observed and calculated patterns, respectively. Tick marks represent calculated peak positions of the main phase (purple) and LaF_3 (orange). The reliability factors are wRp = 5.27% and Rp = 3.99%. (Inset) XRD profiles of the $\{102\}$ and $\{004\}$ peaks of x = 0.1 to 0.8. The dashed lines are guides to the eye.

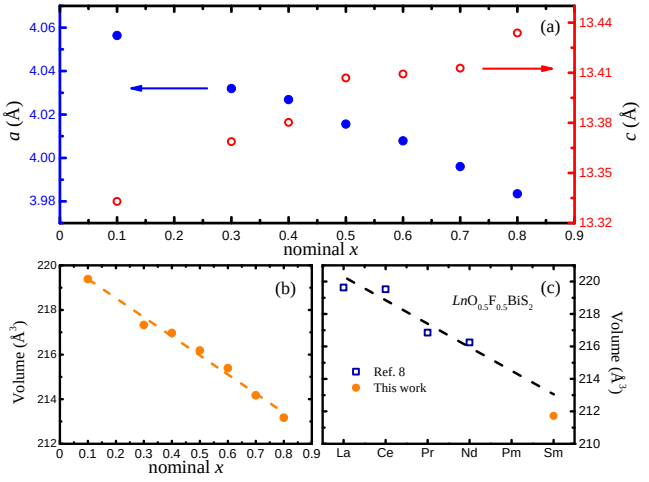

FIG. 2: (Color online) Dependence of (a) lattice parameters a (left axis) and c (right axis), and (b) unit-cell volume V on nominal Sm concentration x. (c) V for $LnO_{0.5}F_{0.5}BiS_2$ (Ln = La, Ce, Pr, Nd) from Ref. 8 and estimated V for $SmO_{0.5}F_{0.5}BiS_2$. Dashed lines are guides to the eye.

Bi_2S_3, but the main impurity in the samples was found to be La(Sm)F_3, typically around 3-5 wt.% for x = 0.1 - 0.7 and around 8 wt.% for x = 0.8 samples. This situation results in a lower fluorine concentration in the main superconducting phase compared with the nominal chemical composition. This is consistent with a very recent study which shows that the actual electron doping level in $LaO_{1-x}F_xBiS_2$ could be much smaller than expected.[16] However, an exact evaluation of the actual chemical composition of the main phase is very difficult due to the multi-phase polycrystalline nature of the samples and the insensitiveness of energy dispersive spectroscopy (EDS) to light elements. To be consistent with previous studies on $LnO_{1-x}F_xBiS_2$, the nominal chemical compositions of the main phase, $La_{1-x}Sm_xO_{1-x}F_xBiS_2$, is used throughout this artical. For $x \geqslant 0.9$, samples contain a considerable amount of impurities and the parent compound $SmO_{0.5}F_{0.5}BiS_2$ could not be synthesized, indicating a Sm solubility limit near 80%.[17] The main diffraction peaks, $\{102\}$ and $\{004\}$, shift with increasing x (see the inset of Fig. 1), indicating a systematic change in the lattice parameters. The Sm concentration dependence of the lattice parameters a, c, and unit-cell volume V for x = 0.1 to 0.8 are summarized in Fig. 2. Although superconductivity is observed in the nominal x = 0.9 sample, its lattice parameters are not plotted here because of the appreciable amount of impurities that make XRD analysis unreliable. As the Sm concentration increases from x = 0.1 to 0.8, the a axis decreases continuously, while the c axis increases, leading to a decrease in unit-cell volume of $\sim$3%. Extrapolation of the unit-cell volume linearly to x = 1 provides an estimated unit-cell volume V = 211.7 Å^3 for $SmO_{0.5}F_{0.5}BiS_2$ (see Fig. 2(c)), which is slightly below an extrapolation of the measured unit-cell volumes for the reported $LnO_{0.5}F_{0.5}BiS_2$ compounds in which the Ln ion is believed to be trivalent.[7]

Electrical resistivity ρ vs. temperature T in zero magnetic field is depicted in Fig. 3. Upon cooling, $\rho(T)$ increases until the onset of the superconducting transition for all samples, indicating semiconducting-like behavior. Previous studies on electrical transport behavior in single crystalline samples of $LnO_{1-x}F_xBiS_2$ (Ln = La, Ce, Nd) do not provide a cohesive or consistent picture of the intrinsic behavior; both metallic and semiconducting-like behavior were observed in these samples depending on the synthesis mothod and the chemical composition.[18,19] Since single crystalline samples of $La_{1-x}Sm_xO_{0.5}F_{0.5}BiS_2$ were not used in this study, it is difficult to determine whether the observed semiconducting-like behavior might be related to poor intergain contact or not. However, if this is a bulk effect in single grains, the samples with higher Sm concentration would have smaller semiconducting energy gaps compared with those with lower Sm concentration since the semiconducting-like behavior is suppressed with Sm substitution.

With Sm substitution for La, the T_c of $La_{1-x}Sm_xO_{0.5}F_{0.5}BiS_2$ gradually increases and reaches a maximum value of $T_{c,\rho}$ = 5.4 K for x = 0.8 as is shown in Fig. 4. The value of $T_{c,\rho}$ is defined by the temperature where the electrical resistivity falls to 50% of its normal-state value, and the width of the transition is characterized by identifying the temperatures where the electrical resistivity decreases to 90% and 10% of that value. For x = 0.9, due to the presence of an appreciable amount of impurities like LaF_3, the actual chemical composition of the sample is probably quite different from the nominal composition (i.e., less fluorine). This would be expected to cause a decrease in T_c,[5] which is consistent with our results. Extrapolating $T_{c,\rho}(x)$ for $x \leqslant 0.8$ linearly to x = 1 yields an estimate for the expected T_c of $SmO_{0.5}F_{0.5}BiS_2$ of $\sim$6.2

K (see Fig. 4), which is significantly higher than the T_c reported for other $LnO_{0.5}F_{0.5}BiS_2$ compounds synthesized at ambient pressure.[7,8] We recently became aware of a report that the parent compound $SmO_{0.5}F_{0.5}BiS_2$ could be synthesized by solid state reaction and it does not exhibit superconductivity above 2 K.[20] However, both this work and a recent study on the system $Nd_{1-z}Sm_zO_{1-y}F_yBiS_2$ show solubility limits of Sm by using the same synthesis method.[17] The T_c of $La_{1-x}Sm_xO_{0.5}F_{0.5}BiS_2$ seems closely related to the lattice parameters shown in Fig. 2(a), which is consistent with the study of the chemical pressure effects on $Ce_{1-x}Nd_xO_{1-y}F_yBiS_2$ and $Nd_{1-z}Sm_zO_{1-y}F_yBiS_2$.[17,21] Besides, the T_c values of $La_{1-x}Sm_xO_{0.5}F_{0.5}BiS_2$ are probably intermediate between those of the parent compounds $LaO_{0.5}F_{0.5}BiS_2$ and $SmO_{0.5}F_{0.5}BiS_2$, otherwise it would be difficult to explain why T_c increases as we substitute non-magnetic La ions by magnetic Sm ions.

The effect of annealing temperature on the electrical resistivity and T_c were also investigated. An annealing temperature of 800°C is suitable to prepare $La_{1-x}Sm_xO_{0.5}F_{0.5}BiS_2$ samples for $x \leqslant 0.3$. However, for $x \geqslant 0.5$, annealing the samples at 800°C caused a significant increase in the amount of impurities, resulting in a large normal-state electrical resistivity and low T_c. To reduce the concentration of these impurities, different heat-treatment temperatures were used to synthesize the samples. By decreasing the annealing temperature, it was possible to significantly enhance T_c and reduce the normal-state electrical resistivity (see Fig. 3(b)) for the samples with high Sm concentrations. On the other hand, when the x = 0.8 sample is annealed at 750°C, T_c is very similar but the electrical resistivity is slightly lower, compared with the T_c and resistivity values for samples annealed at 710°C. This suggests that the optimal annealing temperature for synthesizing $La_{1-x}Sm_xO_{0.5}F_{0.5}BiS_2$ samples with $x \geqslant 0.5$ is probably around 750°C.

Figure 5(a) shows the temperature dependence of zero-field-cooled (ZFC) and field-cooled (FC) dc magnetic susceptibility under an applied magnetic field of 10 Oe. The samples exhibit reasonable diamagnetic signals associated with the induced supercurrent during ZFC measurements, suggesting that the samples are bulk superconductors. A paramagnetic contribution to the magnetic susceptibility around T_c, which is larger at lower external magnetic fields and for higher Sm concentration samples, was observed during both FC and ZFC measurements as shown in Fig. 5(b). Similar features have been reported in certain copper oxide superconductors, Nb disks, MgB_2, and Pb, and are generally referred to as a paramagnetic Meissner effect (PME).[22–27] However, further work needs to be done in order to determine whether the observed paramagnetic signal is associated with the PME or is related to movement of the samples in an inhomogeneous external magnetic field in the MPMS system.[28,29] A jump from negative to positive magnetic susceptibility during ZFC measurements in the data for x = 0.7, 0.8 is an instrumental artifact resulting from a brief loss of the temperature control near the boiling point of ^{4}He, during which the temperature will suddenly increase above T_c and then slowly return to the set point. This induces extra irreversible magnetic flux penetration during ZFC measurements in the samples with $T_c > 4.4$ K. AC magnetic susceptibility data for selected samples with x = 0.1, 0.5, 0.7, and 0.9 are plotted in Figs. 5(c) and (d). The smooth transitions in both ac and dc magnetic susceptibility data imply there is probably only one phase that contributes to the observed bulk shielding signal. No evidence of a structural phase transition induced by Sm substitution was observed.[30–32]

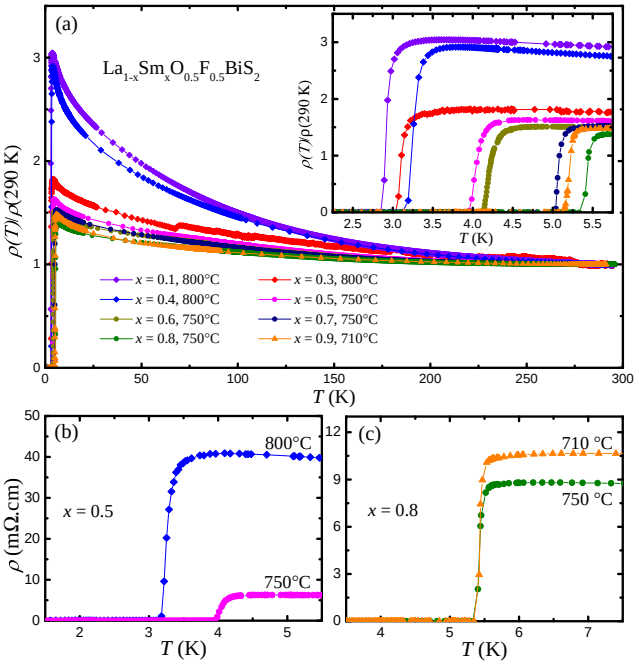

FIG. 3: (Color online) (a) Temperature dependence of the electrical resistivity, $\rho(T)$, normalized by its value at 290 K, ρ(290 K), for $La_{1-x}Sm_xO_{0.5}F_{0.5}BiS_2$. The inset displays the data in panel (a) from 2 to 6 K, emphasizing the superconducting transitions. (b) and (c) Electrical resistivity $\rho(T)$ for two samples with x = 0.5 and x = 0.8, respectively. The annealing temperature used for each sample is denoted.

We defined T_c in dc and ac magnetic susceptibility measurements as the temperature at which the ZFC and FC data separate and the point where the imaginary part drops below zero, respectively. The $T_{c,\chi dc}$ values determined from χ_{dc} measurements increase monotonically from 2.65 K for x = 0.1 to 5.20 K for x = 0.8 as shown in Fig. 4. Furthermore, dc and ac susceptibility measurements reveal enhanced volume and shielding fractions at 2 K with increasing Sm substitution (Fig. 5(e)), respectively, indicating improvements in the quality of the samples. The optimal volume fraction is obtained at x = 0.7. With further Sm substitution, however, the volume fraction rapidly decreases, coinciding with the appearance of an appreciable amount of non-superconducting secondary phases. The fact that the T_c of the sample with x = 0.8 is higher than that of the sample with x = 0.7, which shows the highest volume fraction, implies that superconductivity in $La_{1-x}Sm_xO_{0.5}F_{0.5}BiS_2$ could be further enhanced if samples could be prepared with a higher Sm concentration.

Magnetization M, divided by magnetic field H, M/H, for H

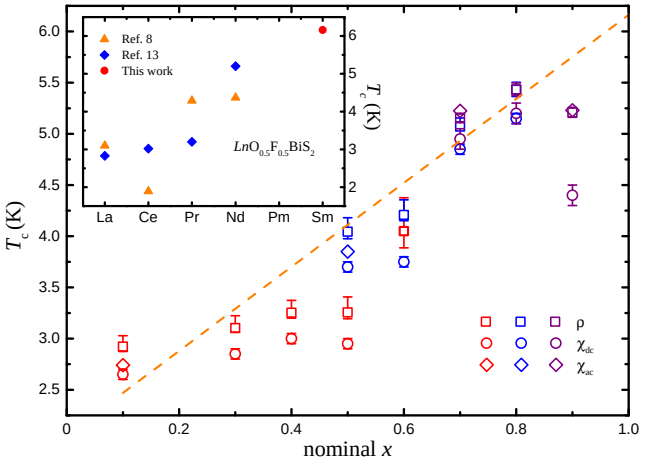

FIG. 4: (Color online) Superconducting critical temperature T_c vs. nominal Sm concentration x of $La_{1-x}Sm_xO_{0.5}F_{0.5}BiS_2$. Red, blue, and purple symbols represent results for samples annealed at 800°C, 750°C, and 710°C, respectively. The dashed line is a linear fit of $T_{c,\rho}$ from x = 0.1 to x = 0.8. (Inset) $T_{c,\rho}$ of $LnO_{0.5}F_{0.5}BiS_2$ compounds reported in Refs. 8 and 13 together with the estimated $T_{c,\rho}$ = 6.2 K of $SmO_{0.5}F_{0.5}BiS_2$.

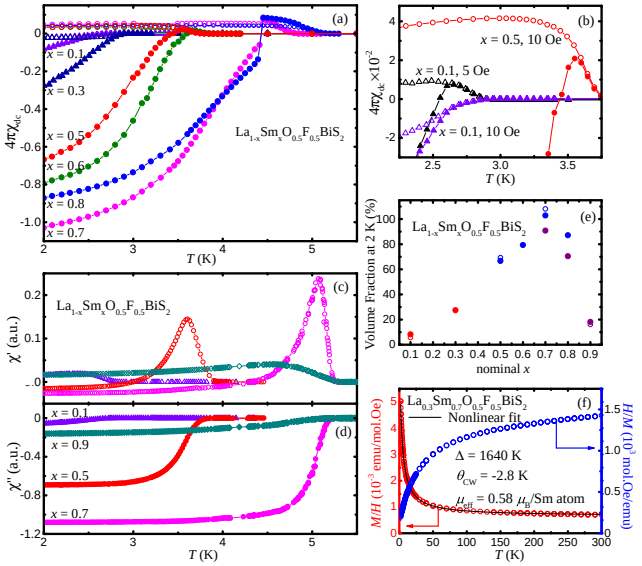

FIG. 5: (Color online) (a) Zero-field-cooled (ZFC) (filled symbols) and field-cooled (FC) (open symbols) dc magnetic susceptibility data for $La_{1-x}Sm_xO_{0.5}F_{0.5}BiS_2$ in an applied magnetic field of 10 Oe. (b) Paramagnetic-like behavior of selected samples with x = 0.1 and 0.9 in applied magnetic fields of 5 Oe and 10 Oe, respectively. Magnetic susceptibility data for x = 0.1 in 10 Oe is also plotted for comparison. (c) Real and (d) imaginary part of the ac magnetic susceptibility for selected samples. (e) Evolution of shielding volume fraction with Sm substitution. Open and filled circles correspond to ac and dc susceptibility; red, blue, and purple colored data points represent measurements on samples annealed at 800°C, 750°C and 710°C, respectively. (f) M/H and H/M vs. T data in the normal state for $La_{0.3}Sm_{0.7}O_{0.5}F_{0.5}BiS_2$, measured from 2 to 300 K in an applied magnetic field of 5 kOe. The solid line is a nonlinear fit using Eq. (1).

= 5 kOe and x = 0.7 is displayed as a function of temperature in Fig. 5(f) (left axis). In addition to distinct non-Curie Weiss behavior (see Fig. 5(f), right axis), there is no evidence for magnetic order down to 2 K. Unlike other heavy lanthanides, the energy between the J = 5/2 ground state and the J = 7/2 first excited state in Sm^{3+} is only 0.12 eV and the Van Vleck term should be considered when modeling the magnetic susceptibility of compounds containing Sm.[33,34] Hence, the temperature dependence of the magnetization was fitted by a modified Curie-Weiss law:

$$\frac{M}{H} = \frac{N_A}{k_B}\left[\alpha_J\mu_B^2 + \frac{\mu_{eff}^2}{3(T-\theta_{CW})}\right], \qquad (1)$$

in which N_A is Avogadro's number, k_B is Boltzmann's constant, μ_B is the Bohr magneton, μ_{eff} is the effective magnetic moment in Bohr magnetons, and θ_{CW} is the Curie-Weiss temperature. We define $\alpha_J = 20/7\Delta$, where Δ is the energy separation between the J = 5/2 ground state multiplet and the J = 7/2 first excited state multiplet for Sm.[35] From the best fit of the M/H data using Eq. (1), values for Δ, θ_{CW}, and μ_{eff} were found to be 1640 K, -2.8 K, and 0.58 μ_B/Sm atom, respectively. The experimental Δ value is close to the estimated value for free Sm^{3+} (∼1500 K).[33] The effective magnetic moment of the samples are considerably smaller than the free Sm^{3+} ion value of 0.845 μ_B/Sm atom. Similar low values of μ_{eff} have been reported in other studies[36,37] and are not necessarily evidence for an intermediate valence for Sm; an accurate theoretical description of experimental data in Sm systems is complicated by the combined effects of the crystalline electric field (CEF) effects and J-mixing.[38]

The results of specific heat C measurements for x = 0.1, 0.8, and a nonmagnetic reference compound $LaOBiS_2$ are displayed in Fig. 6(a), plotted as C/T vs. T. Above 10 K, the specific heat of the compounds are almost the same, due to similar lattice contributions. The upturns in C/T vs. T below 3.7 K and 8.0 K for the samples with x = 0.1 and 0.8, respectively, which overlap with the superconducting transitions, are due to a Schottky contribution (C_{Sch}) caused by CEF splitting of the J = 5/2 Hund's rule ground state multiplet. Hence, the specific heat of the samples consists of electronic (C_{el}), phonon (C_{ph}), and Schottky (C_{Sch}) contributions. The best fit of the $LaOBiS_2$ data below 7 K using $C(T) = C_{el}(T) + C_{ph}(T) = \gamma T + A_3T^3 + A_5T^5$, yields the normal-state electronic specific heat coefficient γ = 3.32 mJ/mol K^2 and the coefficients of the phonon contribution A_3 = 0.655 mJ/mol K^4 and A_5 = 4.27 μJ/mol K^6. Representative (C-C_{ph})/T vs. T data for x = 0.8 are shown in the inset of Fig. 6(a). The phonon contribution of the Sm-substituted samples was assumed to be the same as for $LaOBiS_2$ and was subtracted from the specific heat. The remaining specific heat data could be fitted with the following

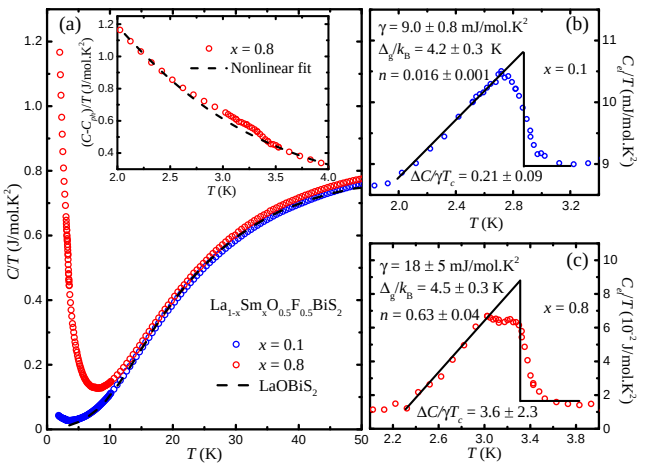

FIG. 6: (Color online) (a) Specific heat C divided by temperature, C/T, vs. T for $La_{1-x}Sm_xO_{0.5}F_{0.5}BiS_2$ with x = 0.1, 0.8 and for $LaOBiS_2$. (Inset) (C-C_{ph})/T vs. T, where C_{ph} is the lattice contribution, and a fit of the Schottky anomaly contribution for $La_{0.2}Sm_{0.8}O_{0.5}F_{0.5}BiS_2$ (dashed line). (b) and (c) Electronic contribution C_{el}/T of $La_{1-x}Sm_xO_{0.5}F_{0.5}BiS_2$ with x = 0.1 and x = 0.8, respectively. An entropy conserving construction is shown, which is used to define T_c.

expression:

$$C(T)/T = \gamma + nC_{Sch}/T = \gamma + n\frac{R}{T}\frac{\left(\frac{\Delta_g}{k_BT}\right)^2 e^{\left(\frac{\Delta_g}{k_BT}\right)}}{\left[1+e^{\left(\frac{\Delta_g}{k_BT}\right)}\right]^2}. \quad (2)$$

The second term in Eq. (2), nC_{Sch}/T, represents a Schottky anomaly in which n is the number of Sm atoms per formula unit that contribute to the Schottky anomaly, Δ_g is the splitting between the ground state and the first excited state doublet of the J = 5/2 Hund's rule ground state multiplet, k_B is Boltzmann's constant, and R is the ideal gas constant. The best fits to the $C(T)/T$ data for the $La_{1-x}Sm_xO_{0.5}F_{0.5}BiS_2$ samples with x = 0.1 and 0.8 provide very similar Δ_g splitting values, but different γ values (listed in Figs. 6(b) and (c)). Subtracting both $C_{ph}(T)$ and $C_{Sch}(T)$ from $C(T)$ data yields the electronic specific heat $C_{el}(T)$ contribution, revealing a clear feature around T_c, which provides evidence for bulk superconductivity.

The electronic contribution to the specific heat data for the x = 0.1 sample shows a jump at ~2.8 K, which is consistent with the T_c obtained from the resistivity and magnetization measurements. However, for the sample with x = 0.8, the T_c values estimated from the entropy conserving-constructions are considerably lower than the $T_{c,\rho}$ values determined from $\rho(T)$ measurements, which may suggest an inhomogeneous distribution of Sm in the polycrystalline samples. Domains with high Sm concentration would result in relatively high T_c values in the electrical resistivity measurement. In contrast, a considerable amount of domains, which are associated with the bulk superconductivty of the sample, could contain a lower Sm concentration with lower T_c. Values of $\Delta C/\gamma T_c$ of 0.21 ± 0.09 and 3.6 ± 2.3 were extracted from the $C_{el}(T)$ data for x = 0.1 and 0.8, respectively. The uncertainties associated with values of γ, Δ_g, n, and $\Delta C/\gamma T_c$, which are shown in Fig. 6(b) and (c), are appreciable for the following reasons. First, making a precise evaluation of the Schottky contribution to the specific heat is very difficult since the local environments of the Sm ions may be quite different due to sample inhomogeneity and the temperatures that have been measured are not low enough to observe the complete profile of the Schottky anomaly. Second, the Schottky contribution to the specific heat at low temperatures is much more significant than the electronic contribution; a slight error in evaluating the Schottky anomaly may result in a considerable uncertainty of the γ value. Third, secondary impurity phases also contribute to the specific heat; however, quantitative analysis of their contributions is very difficult since the amount and exact chemical compositions of these phases are not known with high precision. Finally, there are many variable parameters that are involved in the specific heat analysis, which introduces additional uncertainty into each best-fit value. We estimated the uncertainties associated with the best-fit values for γ, Δ_g, and n by considering both the errors inherent to the specific heat measurements as well as the range of values for γ, Δ_g, and n that lead to optimized fits of the C/T data using Eq. (2). The magnitude of the specific heat jump ΔC at T_c depends sensitively on the values of Δ_g and n since they characterize the large Schottky anomaly contribution to specific heat that is subtracted from the measured C/T data to obtain the electronic contribution C_{el}/T. The uncertainties in the values of $\Delta C/\gamma T_c$ that are presented in Figs. 6(b) and (c) take this into account and are quite large as a consequence. Given the uncertainties involved in the procedure for extracting the $\Delta C/\gamma T_c$ values, these estimates are consistent with bulk superconductivity; however, the question of whether or not the $\Delta C/\gamma T_c$ values of the samples are consistent with the BCS value of 1.43 remains open. To perform a more precise quantitative analysis, homogenous single phase samples of $La_{1-x}Sm_xO_{0.5}F_{0.5}BiS_2$ need to be prepared and the specific heat below 1.8 K should be investigated.

IV. SUMMARY

In summary, the T_c and superconducting volume fraction were found to increase with x in the $La_{1-x}Sm_xO_{0.5}F_{0.5}BiS_2$ samples investigated in the experiments reported herein. The solubility limit of Sm has a large value of $x \sim 0.8$ in $La_{1-x}Sm_xO_{0.5}F_{0.5}BiS_2$, and a continuous decrease in the a axis and increase in the c axis is observed with increasing x. Bulk superconductivity was observed in the samples according to magnetic susceptibility and specific heat measurements. No evidence for a structural phase transition was found in this study. The results demonstrate that the superconducting critical temperature T_c of tetragonal BiS_2-based compounds is correlated with the lattice parameters and can be significantly enhanced by Sm substitution. This gives a promising way to further increase the T_c of BiS_2-based superconductors by modifying the blocking layers through the substitution of

heavier *Ln* lanthanides (*Ln* = Eu - Tm) or synthesizing the parent $LnO_{1-x}F_xBiS_2$ compounds.

Acknowledgments

Research at UCSD was supported by the U. S. Department of Energy, Office of Basic Energy Sciences, Division of Materials Sciences and Engineering under Grant No. DE-FG02-04-ER46105. Helpful discussions about the MPMS measurement artifacts with N. R. Dilley are gratefully acknowledged.

* Corresponding Author: mbmaple@ucsd.edu

1. Y. Mizuguchi, H. Fujihisa, Y. Gotoh, K. Suzuki, H. Usui, K. Kuroki, S. Demura, Y. Takano, H. Izawa, and O. Miura, Phys. Rev. B **86**, 220510 (2012).
2. S. K. Singh, A. Kumar, B. Gahtori, G. Sharma, S. Patnaik, and V. P. S. Awana, J. Am. Chem. Soc. **134**, 16504 (2012).
3. V. P. S. Awana, A. Kumar, R. Jha, S. Kumar Singh, A. Pal, J. Saha, and S. Patnaik, Solid State Commun. **157**, 21 (2013).
4. S. Demura, Y. Mizuguchi, K. Deguchi, H. Okazaki, H. Hara, T. Watanabe, S. James Denholme, M. Fujioka, T. Ozaki, H. Fujihisa, et al., J. Phys. Soc. Jpn. **82**, 033708 (2013).
5. Y. Mizuguchi, S. Demura, K. Deguchi, Y. Takano, H. Fujihisa, Y. Gotoh, H. Izawa, and O. Miura, J. Phys. Soc. Jpn. **81**, 114725 (2012).
6. J. Xing, S. Li, X. Ding, H. Yang, and H.-H. Wen, Phys. Rev. B **86**, 214518 (2012).
7. D. Yazici, K. Huang, B. D. White, A. H. Chang, A. J. Friedman, and M. B. Maple, Phil. Mag. **93**, 673 (2013).
8. Y. Mizuguchi, Physics Procedia **58**, 94 (2014).
9. K. Deguchi, Y. Mizuguchi, S. Demura, H. Hara, T. Watanabe, S. J. Denholme, M. Fujioka, H. Okazaki, T. Ozaki, H. Takeya, et al., Europhys. Lett. **101**, 17004 (2013).
10. R. Jha, A. Kumar, S. K. Singh, and V. P. S. Awana, Journal of superconductivity and novel magnetism **26**, 499 (2013).
11. D. Yazici, K. Huang, B. D. White, I. Jeon, V. W. Burnett, A. J. Friedman, I. K. Lum, M. Nallaiyan, S. Spagna, and M. B. Maple, Phys. Rev. B **87**, 174512 (2013).
12. X. Lin, X. Ni, B. Chen, X. Xu, X. Yang, J. Dai, Y. Li, X. Yang, Y. Luo, Q. Tao, et al., Phy. Rev. B **87**, 020504 (2013).
13. V. S. Tanryverdiew, O. M. Aliew, and I. I. Aliev, Inorg. Mater. **31**, 1361 (1995).
14. A. C. Larson and R. B. Von Dreele, Los Alamos National Laboratory Report (1994).
15. B. H. Toby, J. Appl. Crystallogr. **34**, 210 (2001).
16. Z. R. Ye, H. F. Yang, D. W. Shen, J. Jiang, X. H. Niu, D. L. Feng, Y. P. Du, X. G. Wan, J. Z. Liu, X. Y. Zhu, et al., Phys. Rev. B **90**, 045116 (2014).
17. J. Kajitani, T. Hiroi, A. Omachi, O. Miura, and Y. Mizuguchi, arXiv preprint arXiv:1408.2625 (2014).
18. M. Nagao, A. Miura, S. Demura, K. Deguchi, S. Watauchi, T. Takei, Y. Takano, N. Kumada, and I. Tanaka, Solid State Commun. **178**, 33 (2014).
19. X. B. Wang, S. M. Nie, H. P. Wang, P. Zheng, P. Wang, T. Dong, H. M. Weng, and N. L. Wang, Phys. Rev. B **90**, 054507 (2014).
20. G. S. Thakur, G. K. Selvan, Z. Haque, L. C. Gupta, S. L. Samal, S. Arumugam, and A. K. Ganguli, arXiv preprint arXiv:1410.0751 (2014).
21. J. Kajitani, A. Omachi, T. Hiroi, O. Miura, and Y. Mizuguchi, Physica C **504**, 33 (2014).
22. I. A. Chaban, J. Supercond. **13**, 1011 (2000).
23. D. J. Thompson, M. S. M. Minhaj, L. E. Wenger, and J. T. Chen, Phys. Rev. Lett. **75**, 529 (1995).
24. W. Braunisch, N. Knauf, V. Kataev, S. Neuhausen, A. Grütz, A. Kock, B. Roden, D. Khomskii, and D. Wohlleben, Phys. Rev. Lett. **68**, 1908 (1992).
25. H. Sözeri, L. Dorosinskii, U. Topal, and I. Ercan, Physica C **408**, 109 (2004).
26. S. Yuan, L. Ren, and F. Li, Phys. Rev. B **69**, 092509 (2004).
27. E. L. Papadopoulou, P. Nordblad, P. Svedlindh, R. Schöneberger, and R. Gross, Phys. Rev. Lett. **82**, 173 (1999).
28. T. P. Papageorgiou, H. F. Braun, and T. Herrmannsdörfer, Phys. Rev. B **66**, 104509 (2002).
29. M. McElfresh, S. Li, and R. Sager, Quantum Design (San Diego) technical report (1996).
30. Y. Mizuguchi, T. Hiroi, J. Kajitani, H. Takatsu, H. Kadowaki, and O. Miura, J. Phys. Soc. Jpn. **83**, 053704 (2014).
31. H. Kotegawa, Y. Tomita, H. Tou, H. Izawa, Y. Mizuguchi, O. Miura, S. Demura, K. Deguchi, and Y. Takano, J. Phys. Soc. Jpn. **81**, 103702 (2012).
32. C. T. Wolowiec, B. D. White, I. Jeon, D. Yazici, K. Huang, and M. B. Maple, J. Phys.: Condens. Matter **25**, 422201 (2013).
33. J. H. Van Vleck, *The theory of electric and magnetic susceptibilities*, vol. 72 (Oxford University Press London, 1965).
34. M. B. Maple, in *High-Pressure and Low-Temperature Physics* (Springer, 1978).
35. D. Wagner, *Introduction to the Theory of Magnetism*, vol. 48 (Pergamon, 1972).
36. M. B. Maple and D. Wohlleben, Phys. Rev. Lett. **27**, 511 (1971).
37. K. Ahn, V. K. Pecharsky, and K. A. Gschneidner, Phys. Rev. B **76**, 014415 (2007).
38. K. A. Gschneidner, L. Eyring, and G. H. Lander, *Handbook on the physics and chemistry of rare earths*, vol. 32 (Elsevier, 2001).